Exchange bias in $La_{0.7}Sr_{0.3}CrO_3/La_{0.7}Sr_{0.3}MnO_3/La_{0.7}Sr_{0.3}CrO_3$ heterostructures

Rubyann Olmos,[1] Hector Iturriaga,[1] Dawn S. Blazer,[1] Sanaz Koohfar,[3] Kinjal Gandha,[2] Ikenna C. Nlebedim,[2] Divine P. Kumah,[3] and Srinivasa R. Singamaneni[1,a*]

[1]*Department of Physics, University of Texas at El Paso, El Paso, Texas 79968, USA*

[2]*Critical Materials Institute, Ames Laboratory, 311 Iowa State University, Ames, Iowa 50011, USA*

[3]*Department of Physics, North Carolina State University, Raleigh, North Carolina 27695, USA*

In the recent past, heterostructures of magnetic oxide thin films have attracted a great deal of research excitement due to very interesting physical properties such as antiferromagnetic interlayer coupling, tunable exchange-bias, interfacial driven magnetic properties and high mobility electron gas across the interfaces. In this work, we report on the comprehensive magnetic properties observed from the heterostructures of (2 unit cells) $La_{0.7}Sr_{0.3}CrO_3$/(8 unit cells) $La_{0.7}Sr_{0.3}MnO_3$/(2 unit cells) $La_{0.7}Sr_{0.3}CrO_3$, which are epitaxially deposited on $SrTiO_3$ substrate by plasma-assisted oxide molecular beam epitaxy. Using SQUID magnetometer, the magnetic properties are studied when the magnetic field was applied both in plane and out of plane. The Curie temperature of this structure is found to be at 290 K. Most significantly, at 2 K, we observed a complete up/down shift (along magnetization axis) of hysteresis loop when the sample was cooled under a magnetic field of ± 5000 Oe in the in-plane configuration. We believe that the strong antiferromagnetic (super) exchange coupling of Mn-Cr across the two interfaces is responsible for the observed exchange bias. We will present and discuss our in-detailed experimental findings collected on this heterostructure as a function of temperature and magnetic field.

I. INTRODUCTION

Transition metal oxides (TMOs) are a group of compounds of increasing interest due to properties that make them prospective candidates for engineering applications and technologies. TMO heterostructures portray interesting physical phenomena often not seen in their bulk counterparts such as interactions of atoms at the interface and across the boundary, reduced site coordination of lattice atoms at interface, and a break in translational symmetry of crystal potential.[1] TMO thin films, heterostructures ranging from micro- (10^{-6} m) to nano-meters (10^{-9} m) in thickness, display interfacial interactions that

[a] Corresponding author. Electronic mail: srao@utep.edu*

can lead to effects such as antiferromagnetic interlayer coupling, tunable exchange bias, thickness dependent phase transitions, and high mobility of two-dimensional electron gas across interfaces.[2-4] The interfacial interactions leading to such phenomena stem from interactions occurring with lattice, charge, orbitals and spins giving rise to a sensitivity to strain, electric and magnetic fields, as well as chemical doping.[5] Moreover, with these interesting properties, including magnetoresistance and half-metallic properties, TMO thin films can be applied towards applications in spintronics, magnetic sensors, and magnetic random-access memory [1,6]. However, with the reconstruction of the structure occurring at the interface, a strong thickness dependent property arises which in turn has led to a surge in researchers searching to find ways to control these properties.

Particularly, $LaSrMnO_3$, or LSMO films are of interest as they exhibit attractive properties as mentioned before such as colossal magnetoresistance and half-metallicity. LSMO can be coupled with other TMOs such as $LaSrCrO_3$. The tri-layer thin film $La_{0.7}Sr_{0.3}CrO_3/La_{0.7}Sr_{0.3}MnO_3/La_{0.7}Sr_{0.3}CrO_3$ (LSCO/LSMO/LSCO) consists of an anti-ferromagnetic (AFM) surface layer—where Cr and Mn ions exhibit an AFM exchange interaction—that is situated between two robust anti-ferromagnetic (AFM) layers of LSCO that allow the LSMO layer to retain its ferromagnetic properties.[3] Along with the FM and AFM exchange coupling are the effects of enhanced coercivity and asymmetry in magnetization reversal processes.[7-9] Moreover, many of these exchange bias effects have occurred in other thin film systems.[10-13] In this work, we will present on the magnetic properties of $La_{0.7}Sr_{0.3}CrO_3/La_{0.7}Sr_{0.3}MnO_3/La_{0.7}Sr_{0.3}CrO_3$ epitaxially deposited on a $SrTiO_3$ (STO) substrate, including exchange bias as a function of temperature and magnetic field.

II. EXPERIMENTAL DETAILS

A. Heterostructure synthesis

The thin film was synthesized by plasma-assisted oxide molecular beam epitaxy and consists of two layers of $La_{0.7}Sr_{0.3}CrO_3$ (LSCO) that are 2 unit cells in thickness and a layer of $La_{0.7}Sr_{0.3}MnO_3$ (LSMO) 8 unit cells thick.[3] The layering of the thin film consisted of a LSMO layer sandwiched between LSCO layers epitaxially deposited in an (001) orientation of a $SrTiO_3$ substrate at a growth temperature of 800 °C. The LSCO and LSMO layers were grown in $3x10^{-6}$ Torr atomic oxygen from the plasma source. The sample was cooled down at a rate of 5 °C/min in $5x10^{-6}$ Torr oxygen to ensure that full oxidation occurred. The dimensions of the heterostructure are approximately 3.9 mm by 3.8 mm.

B. Magnetic measurements

Magnetic properties were measured with Quantum Design's MPMS 3 Superconducting Quantum Interference Device (SQUID) using Vibrating Sample Magnetometer option. Temperature dependent measurements were done with a

temperature range of 2-400 K with a measuring field of 500 Oe for zero-field cool (ZFC) and field cool (FC) and an applied field of 200 Oe for FC. Isothermal magnetization was measured between 2-350 K and at ± 5000 Oe in different configurations where the magnetic field was applied in-plane, 90° rotated in-plane, and out-of-plane. For in-plane measurements, the thin film was mounted on a flat quartz rod; for out-of-plane sample was inserted and held in place in a plastic straw provided by Quantum Design. The resulting magnetic measurements have a small diamagnetic signal arising from the STO substrate. In separate measurements, the diamagnetic signal has been subtracted for data seen in Fig. 1(a) and 3(a) confirming that the diamagnetic contribution does not significantly affect the overall magnetic behavior we observe for LSCO/LSMO/LSCO. Therefore, figures containing magnetic data are not refined with diamagnetic subtraction, however, it can be concluded that an accurate representation of the magnetic behavior of LSCO/LSMO/LSCO is observed nonetheless.

III. RESULTS AND DISCUSSION

To begin magnetic measurements, the sample is heated to 400 K to the paramagnetic phase of the thin film as the expected Curie temperature (T_C) is 290 K. Temperature dependent (M-T) measurements are seen in Figure 1(a), where T_C can be estimated from the derivative of magnetic moment with respect to temperature. In both ZFC and FC curves, we see an unexpected spike in the curves at approximately 54 K. The significance of this spike seemingly stems from the cooling of adsorbed oxygen on the sample surface which represents a paramagnetic to AFM transition of oxygen approximately between 52-55 K as explained in T. Dubroca *et al.*[14] In the M-T plots (Fig. 1(a)), it is confirmed that the samples magnetic moment is field dependent at a FC of 200 Oe and increases upon cooling with the application of an external field.

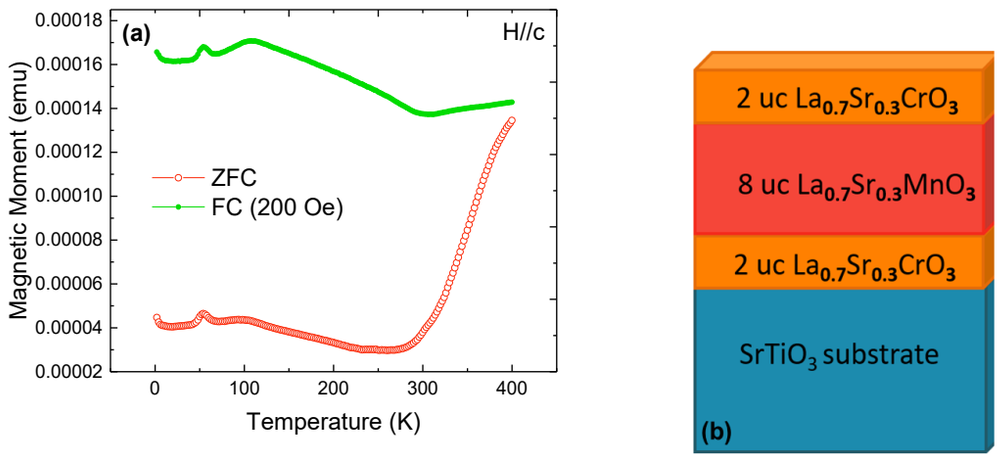

FIG. 1. (a) ZFC and FC (H = 200 Oe) curves measured at a field of 500 Oe for in plane (H//c) measurements between 2-400 K. (b) A schematic of the LSCO/LSMO/LSCO heterostructure on $SrTiO_3$ substrate is shown.

The next set of measurements are magnetic moment versus magnetic field (M-H), are between 2 to 350 K with no applied external field. An interesting phenomena occurs with in-plane data particularly for hysteresis loops above the T_C measured at

300 and 350 K. Asymmetry and a broad hysteresis loop is observed for these temperatures and can be seen in Figure 2(a) and (b), suggesting an exchange bias effect possibly arising from the different magnetic phases of LSCO/LSMO/LSCO. Furthermore, for these M-H curves, the hysteresis loops do not completely saturate. In order to see if full saturation can be achieved and to rule out any artifact(s), test measurements are completed at 300 K at 10,000 Oe. It is observed that the loop still does not fully saturate with the application of set field and even more a possible training effect is noticed on the exchange bias additionally ruling out any artifact occurring with the measurement. The training effect is the gradual and monotonous degradation of the exchange bias shift along the field axis upon cycles that the system is going through with consecutive hysteresis loops at a fixed temperature, such as seen here at 300 K.[15] In Figure 2(c), an overall decrease in hysteresis loop is visible when the second run of the loop is measured. When comparing the coercive field (H_c) of each sweep to determine the exact units the loops have shifted the first sweep's left-most H_c to be -4267.85 Oe and the second sweep's H_c = -2748.93. The right-most H_c for both sweeps are relatively close at 1201 Oe and 1318 Oe, for the first and second sweeps, respectively. Figure 2(d) displays the configuration of 90° in-plane for temperatures at 2 and 300 K. A diamagnetic signal is seen in the hysteresis loop at 300 K; however, a magnetic phase transition is still evident.

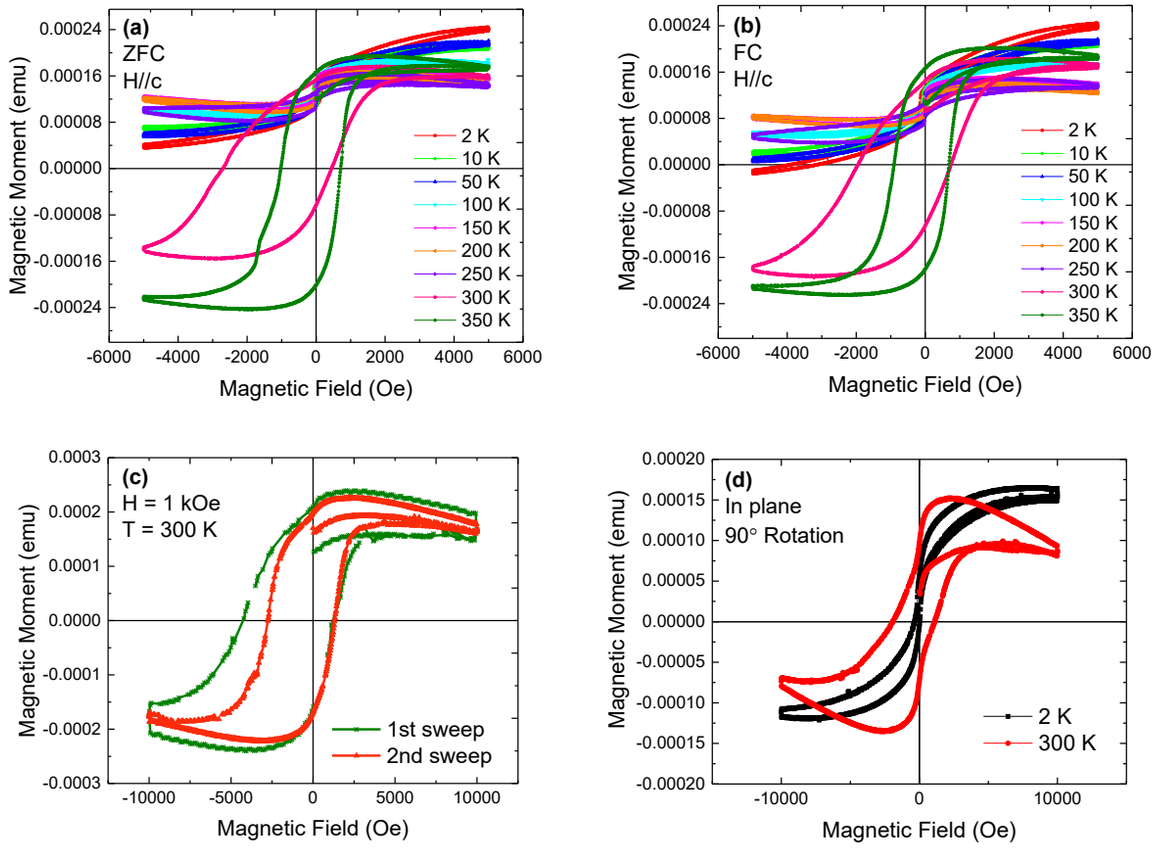

FIG. 2. In-plane magnetic moment versus magnetic field for temperatures at 2-350 K for (a) ZFC and (b) FC. (c) M-H testing at 300 K with an applied magnetic field of 1 T. (d) M-H hysteresis loops at 2 and 300 K for in-plane 90° rotation configuration.

In Figure 3(a), the 90° in-plane rotation FC data is shown at 2 K with ± 0.5 T field. The observation is that there is a clear shift in the hysteresis loops for (+) 5,000 Oe and (-) 5,000 Oe. Moreover, it can be inferred that Figure 3(a)(b) shows the field dependence of LSCO/LSMO/LSCO for out-of-plane and in-plane configurations, as there is evidence of a predominant upward shift on the magnetic moment axis for the in-plane configuration with a FC of (+) 5000 Oe (Fig 3(a)). Furthermore, in magnetic field dependent measurements the saturation of the moment does not occur even at the maximum applied magnetic field 10,000 Oe. Magnetic anisotropy is also observed from comparing the hysteresis loop shapes of the three configurations at which the measurements were done. Additionally, it is found that the magnetic easy axis lays along the in-plane configuration.

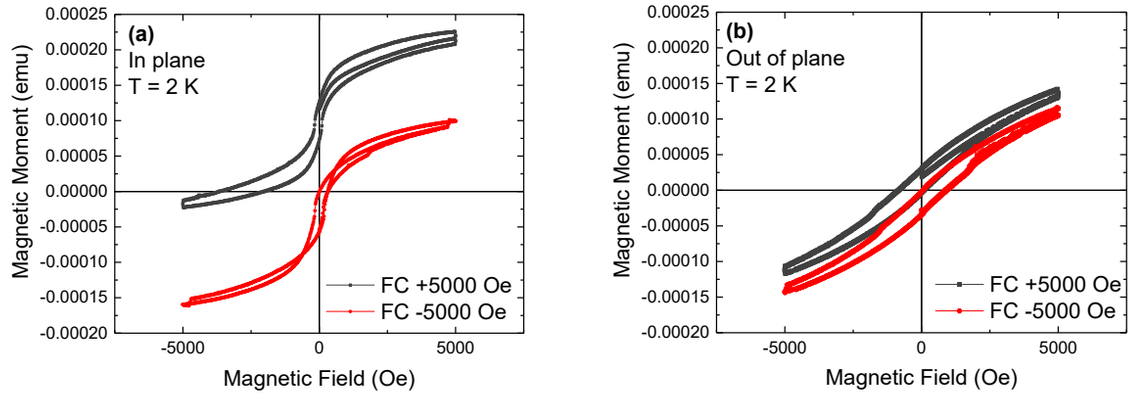

FIG. 3. M-H FC loops at ± 5,000 Oe for (a) in-plane and (b) out-of-plane configurations at T = 2 K showing vertical (a) and horizontal (b) shifts of the magnetic hysteresis loops.

IV. CONCLUSION

The magnetic properties of LSCO/LSMO/LSCO deposited on STO have shown effects such as anti-ferromagnetic exchange coupling, exchange bias observed through asymmetry and a shift on the magnetic moment axis, and an indication of magnetic anisotropy. A possible training effect has also been observed at 10,000 Oe and will need more investigation to completely comprehend the cyclability of the thin film. Additionally, it is believed that the strong anti-ferromagnetic (super) exchange coupling of Mn-Cr across the interfaces is responsible for the exchange bias observation.

The training effect phenomena observed at 300 K may be worth investigating in order to determine the number of cycles the thin film will undergo until returning to the original cycle. Future work may include taking steps toward completing structural characterization methods to further confirm the origin of the interactions observed and exact composition of the thin film. Several prospective measurements will take place with aberration corrected high-angle annular dark-field scanning,

transmission electron microscopy (TEM), electron energy loss spectroscopy (EELS), and energy dispersive x-ray spectroscopy chemical mapping in order to confirm unit cell layer thicknesses of the thin film and the valence states of elements in the layers.

V. ACKNOWLEDGMENTS

This work is supported by the Critical Materials Institute (CMI), an Energy Innovation Hub funded by the U.S. Department of Energy (DOE), Office of Energy Efficiency and Renewable Energy, Advanced Manufacturing Office. Ames Laboratory is operated for the U.S. Department of Energy by Iowa State University of Science and Technology under Contract No. DE-AC02-07CH11358. R.O., H.I., D.S.B., S.R.S. acknowledge support by the National Science Foundation (NSF) Louis Stokes Alliance for Minority Participation (LSAMP) Program under Grant No. NSF HRD-1826745. Material synthesis is supported by the US National Science Foundation under Grant No. NSF DMR-1751455. R.O., H.I., S.R.S. acknowledge Nuclear Regulatory Commission (31310018M0019). The statements, findings, conclusions, and recommendations are those of the author(s) and do not necessarily reflect the view of (UTEP) or The Nuclear Regulatory Commission.

VI. REFERENCES

[1] C. A. F. Vaz, F. J. Walker, C. H. Ahn, and S. Ismail-Beigi. Journal of Physics: Condensed Matter, 27 123001 (2015).
[2] S. Stemmer and S. J. Allen. Annual Review of Materials Research, 44:151-171 (2014).
[3] S. Koohfar, A. B. Georgescu, A. N. Penn, J. M. LeBeau, E. Arenholz, and D. P. Kumah. npj Quantum Materials, 4:25 (2019).
[4] B. Li, R. V. Chopdekar, A. T. N'Diaye, A. Mehta, J. P. Byers, N. D. Browning, E. Arenholz, Y. Takamura. Applied Physics Letters, 109 152401 (2016).
[5] P. Zubko, S. Gariglio, M. Gabay, P. Ghosez, and J. M. Triscone. Annual Review of Materials Research, 2:141-165 (2011).
[6] M. Bibes, J. E. Villegas, A. Barthelemy. Advances in Physics, 60:1, 5-84 (2011).
[7] J. Camarero, Y. Pennec, J. Vogel, S. Pizzini, M. Cartier, F. Fettar, F. Ernult, A. Tagliaferri, N.B. Brookes, and B. Dieny, Phys. Rev. B 67 (2) 020413 (2003).
[8] J. Camarero, J. Sort, A. Hoffmann, J.M. García-Martín, B. Dieny, R. Miranda, J. Nogués, Phys. Rev. Lett. 95 (5) 057204 (2005).
[9] A. Tillmanns, S. Oertker, B. Beschoten, G. Güntherodt, J. Eisenmenger, I.K. Schuller, Phys. Rev. B 78 (1) 012401 (2008).
[10] S. Maat, K. Takano, S.S.P. Parkin, E.E. Fullerton, Phys. Rev. Lett. 87 (8) 087202 (2001).
[11] A.K. Suszka, O. Idigoras, E. Nikulina, A. Chuvilin, A. Berger, Phys. Rev. Lett. 109 (17) (2012).
[12] F. Radu, M. Etzkorn, R. Siebrecht, T. Schmitte, K. Westerholt, H. Zabel, Phys. Rev. B 67 (13) 134409 (2003).
[13] J. Nogués, J. Sort, V. Langlais, V. Skumryev, S. Suriñach, J.S. Muñoz, M.D. Baró, Phys. Rep. 422 (3) 65–117 (2005).
[14] T. Dubroca, J. Hack, R. Hummel, Phys. Rev. B 74, 026403 (2006).
[15] J. Nogues and I. K. Schuller. Journal of Magnetism and Magnetic Materials, 192 203-232 (1999).

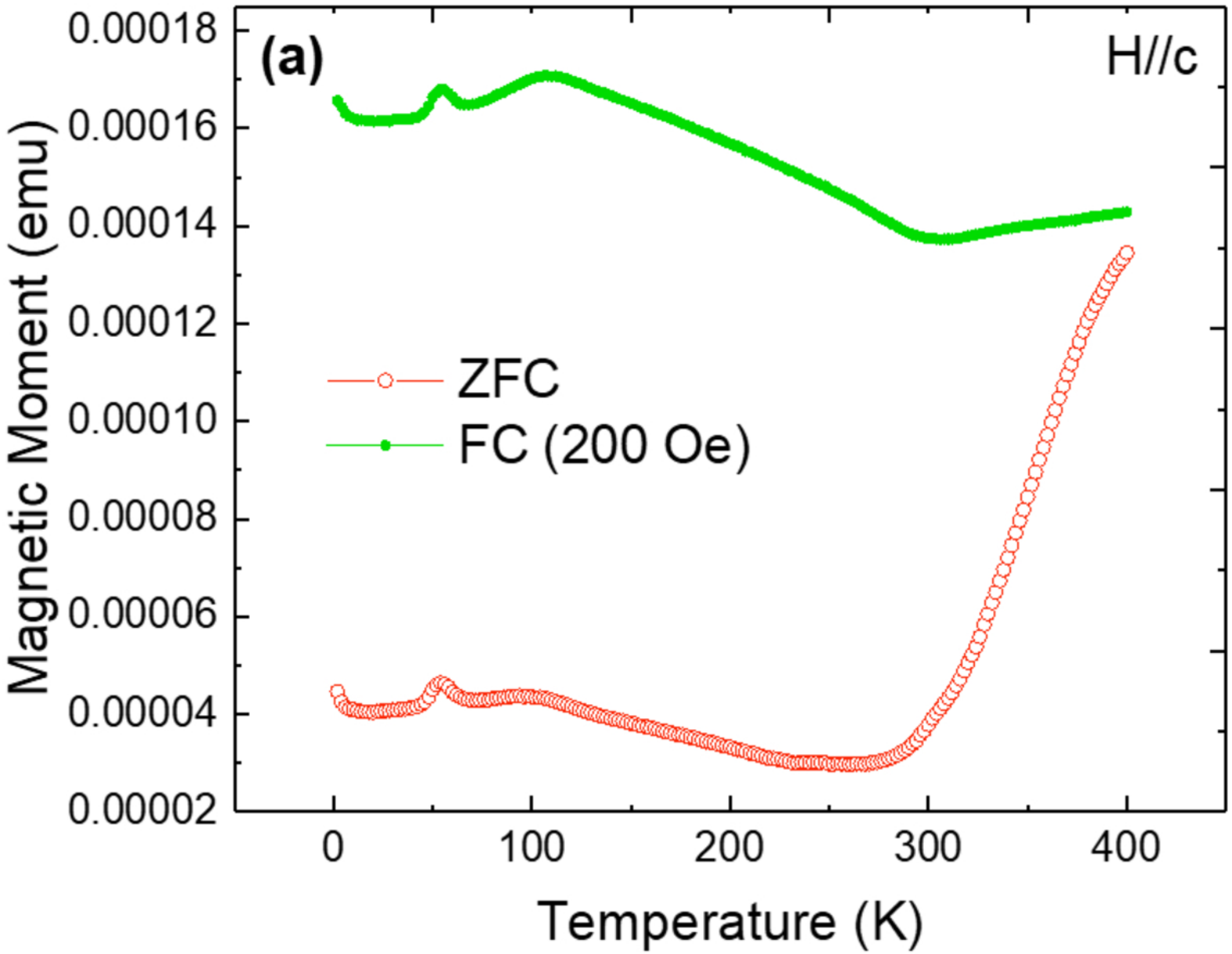
(a)
H//c
ZFC
FC (200 Oe)
Magnetic Moment (emu)
0.00018
0.00016
0.00014
0.00012
0.00010
0.00008
0.00006
0.00004
0.00002
0
100
200
300
400
Temperature (K)

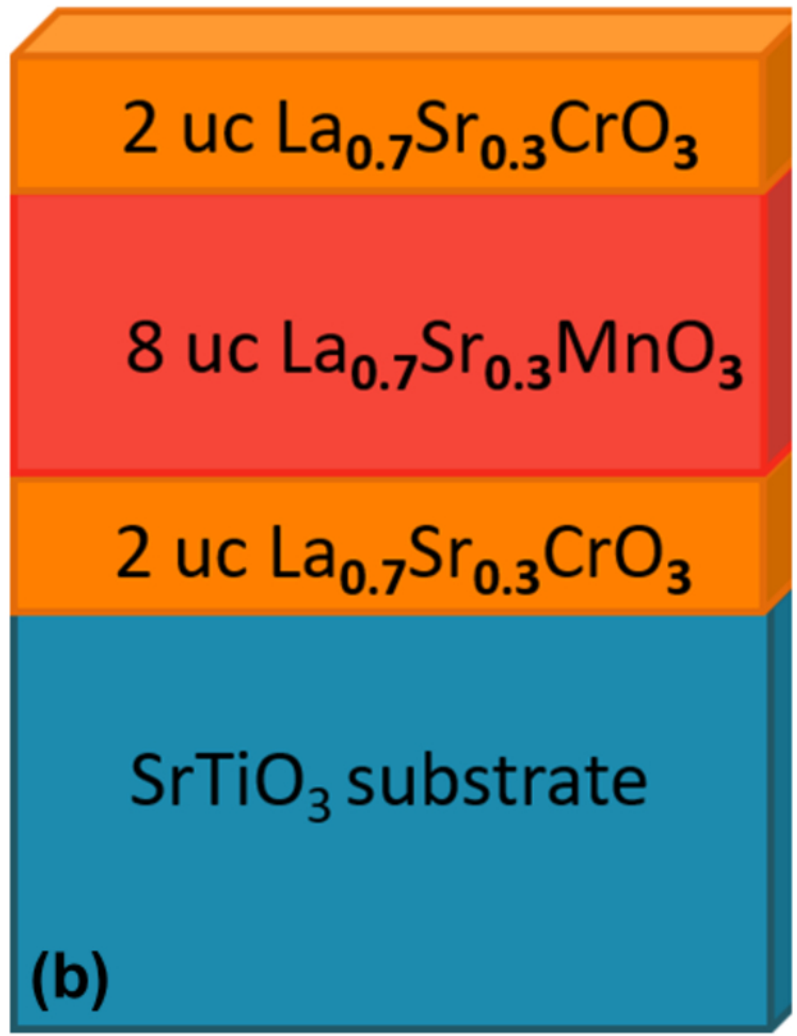
2 uc $La_{0.7}Sr_{0.3}CrO_3$
8 uc $La_{0.7}Sr_{0.3}MnO_3$
2 uc $La_{0.7}Sr_{0.3}CrO_3$
$SrTiO_3$ substrate
(b)

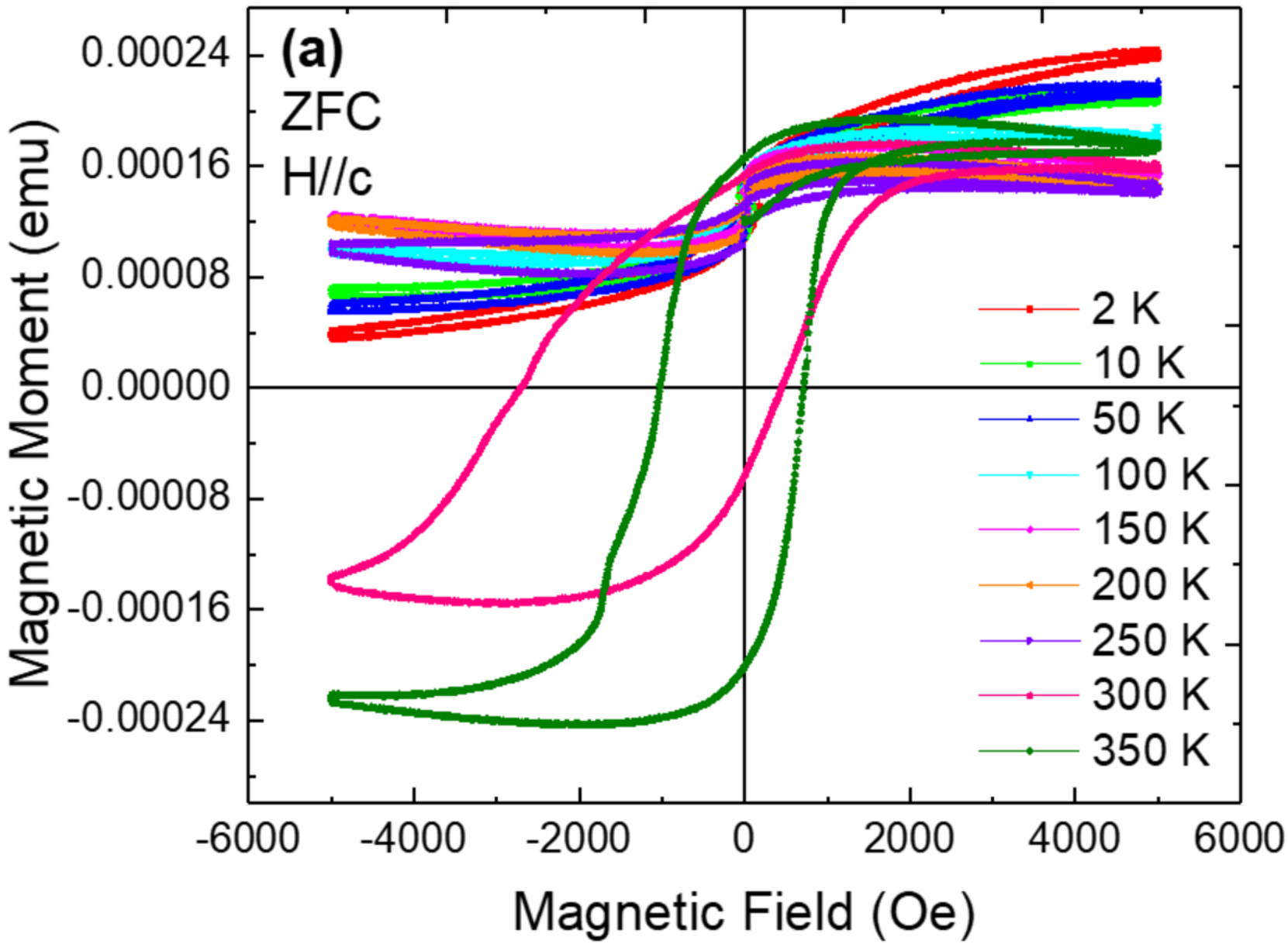
(a)
ZFC
H//c
0.00024
0.00016
0.00008
0.00000
-0.00008
-0.00016
-0.00024
Magnetic Moment (emu)
-6000
-4000
-2000
0
2000
4000
6000
Magnetic Field (Oe)
2 K
10 K
50 K
100 K
150 K
200 K
250 K
300 K
350 K

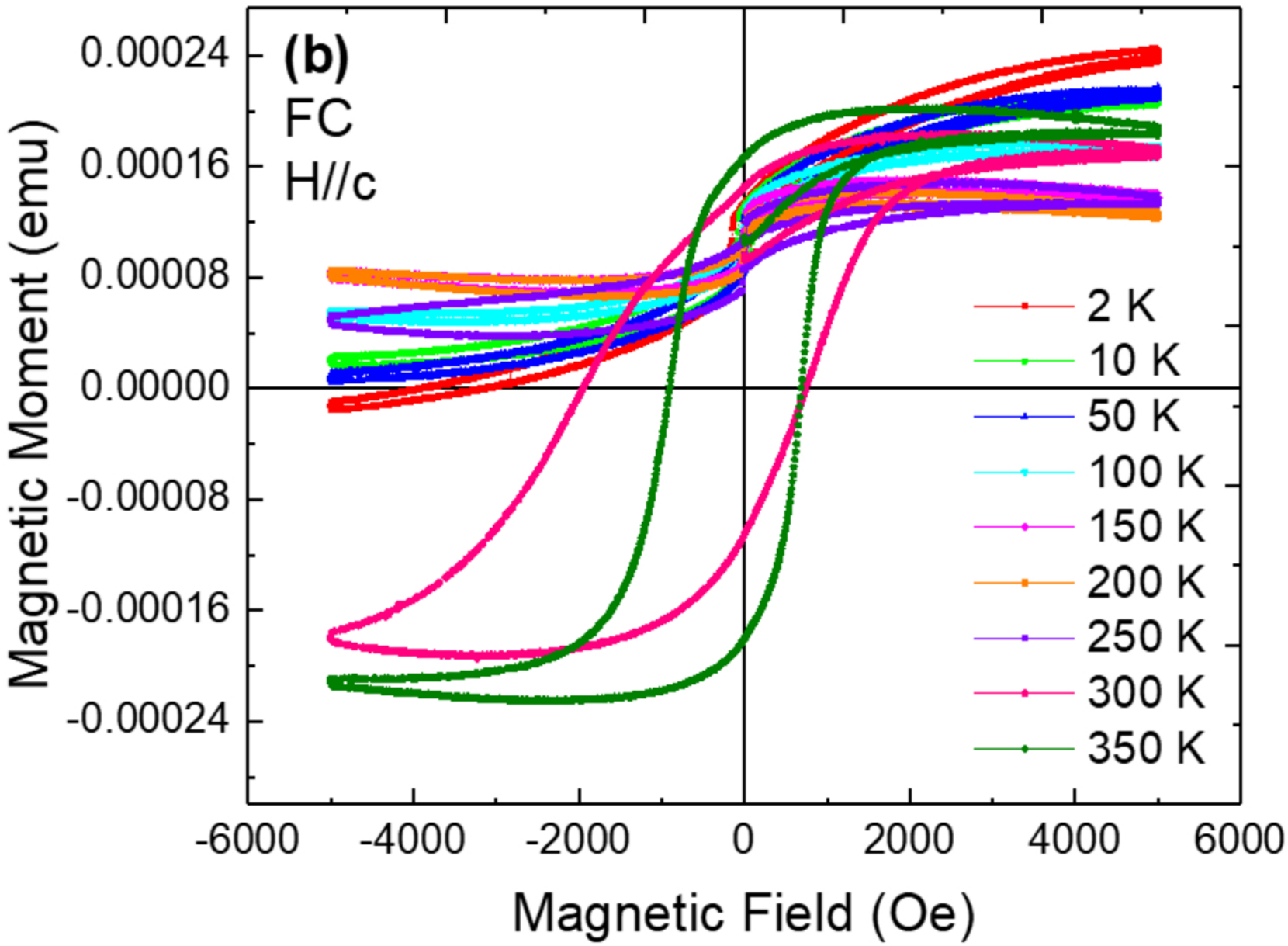
(b)
FC
H//c
0.00024
0.00016
0.00008
0.00000
-0.00008
-0.00016
-0.00024
Magnetic Moment (emu)
-6000
-4000
-2000
0
2000
4000
6000
Magnetic Field (Oe)
2 K
10 K
50 K
100 K
150 K
200 K
250 K
300 K
350 K

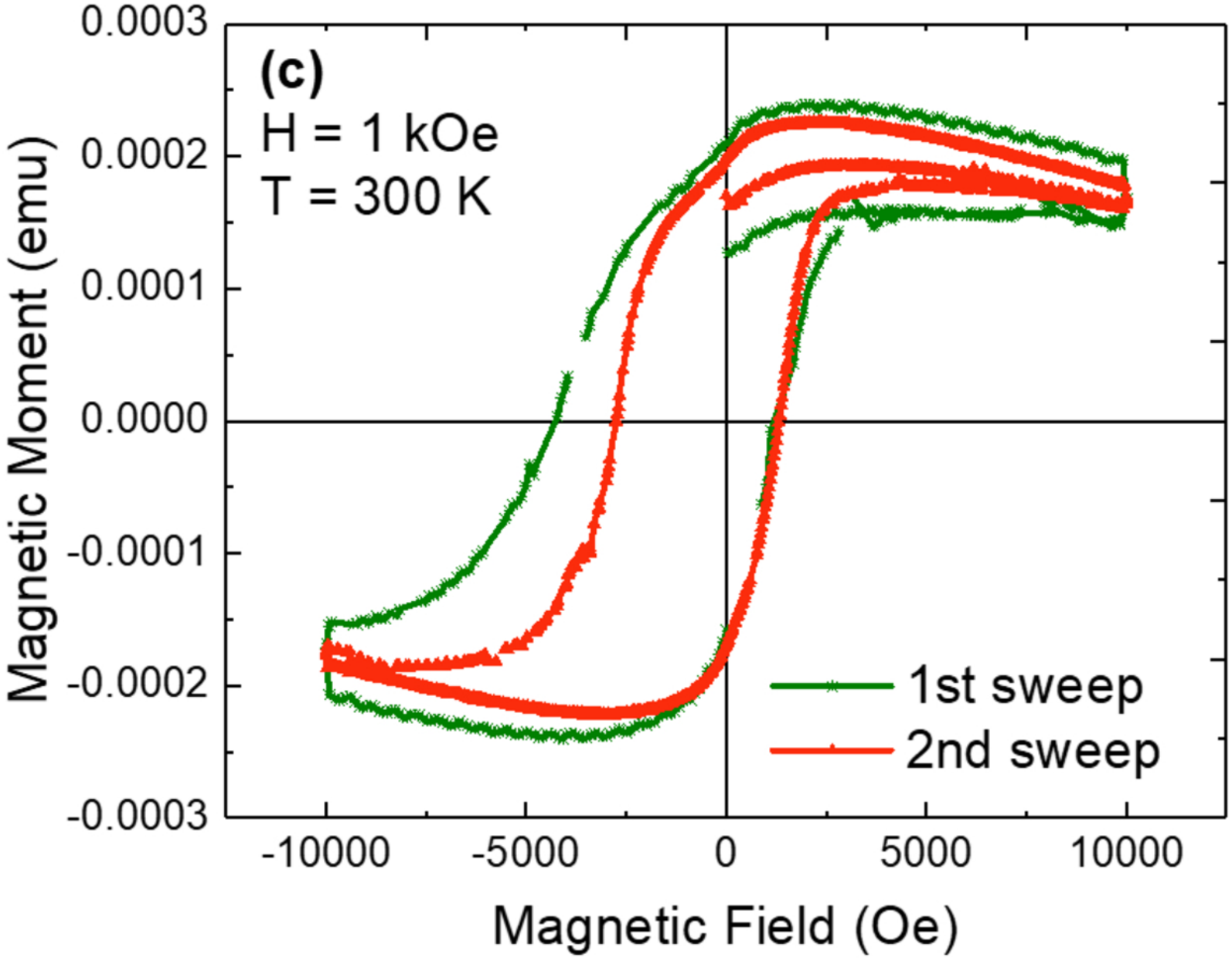
(c)
H = 1 kOe
T = 300 K
1st sweep
2nd sweep
Magnetic Moment (emu)
Magnetic Field (Oe)
0.0003
0.0002
0.0001
0.0000
-0.0001
-0.0002
-0.0003
-10000
-5000
0
5000
10000

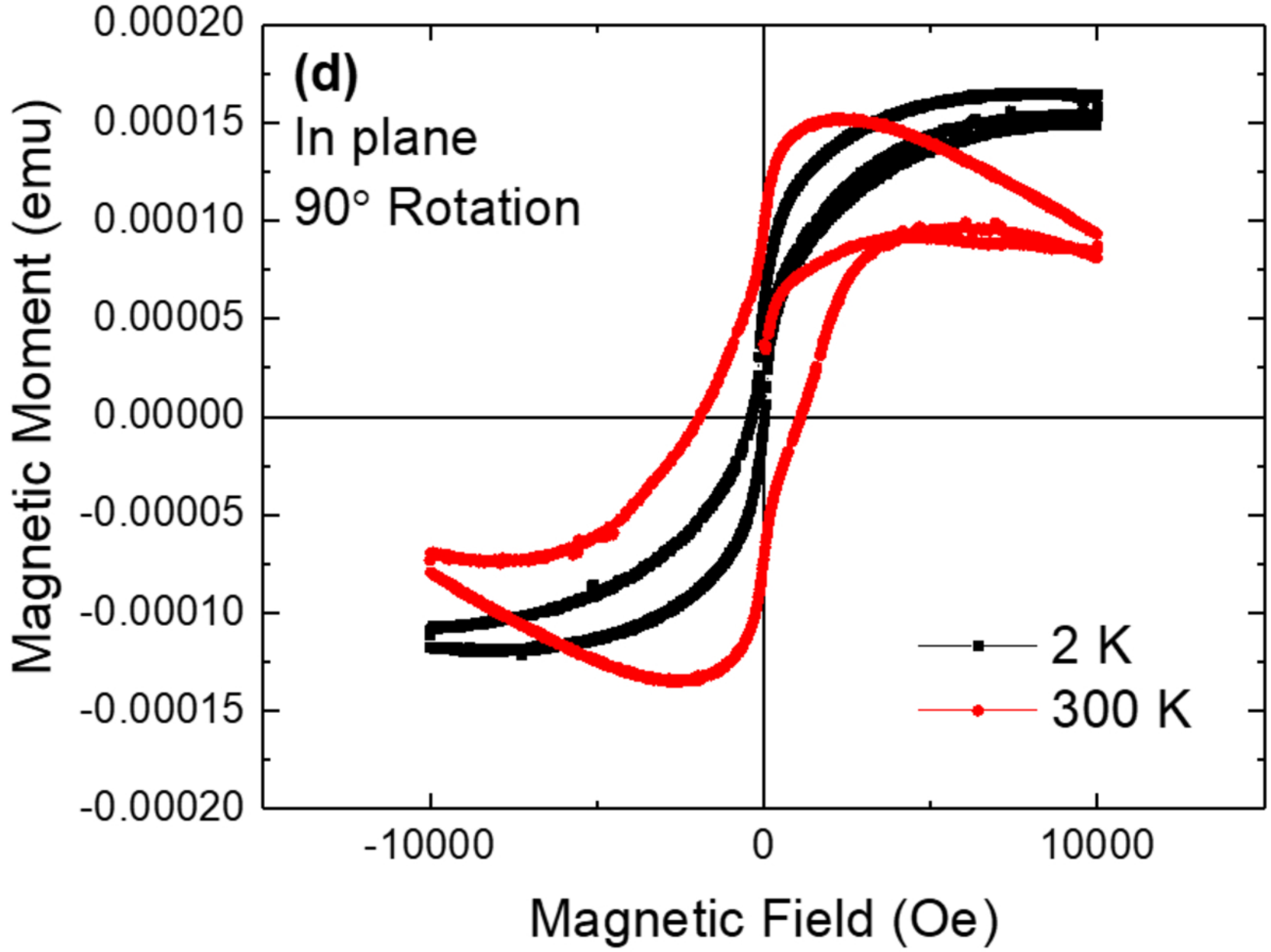
(d)
In plane
90° Rotation
2 K
300 K
Magnetic Moment (emu)
Magnetic Field (Oe)
0.00020
0.00015
0.00010
0.00005
0.00000
-0.00005
-0.00010
-0.00015
-0.00020
-10000
0
10000

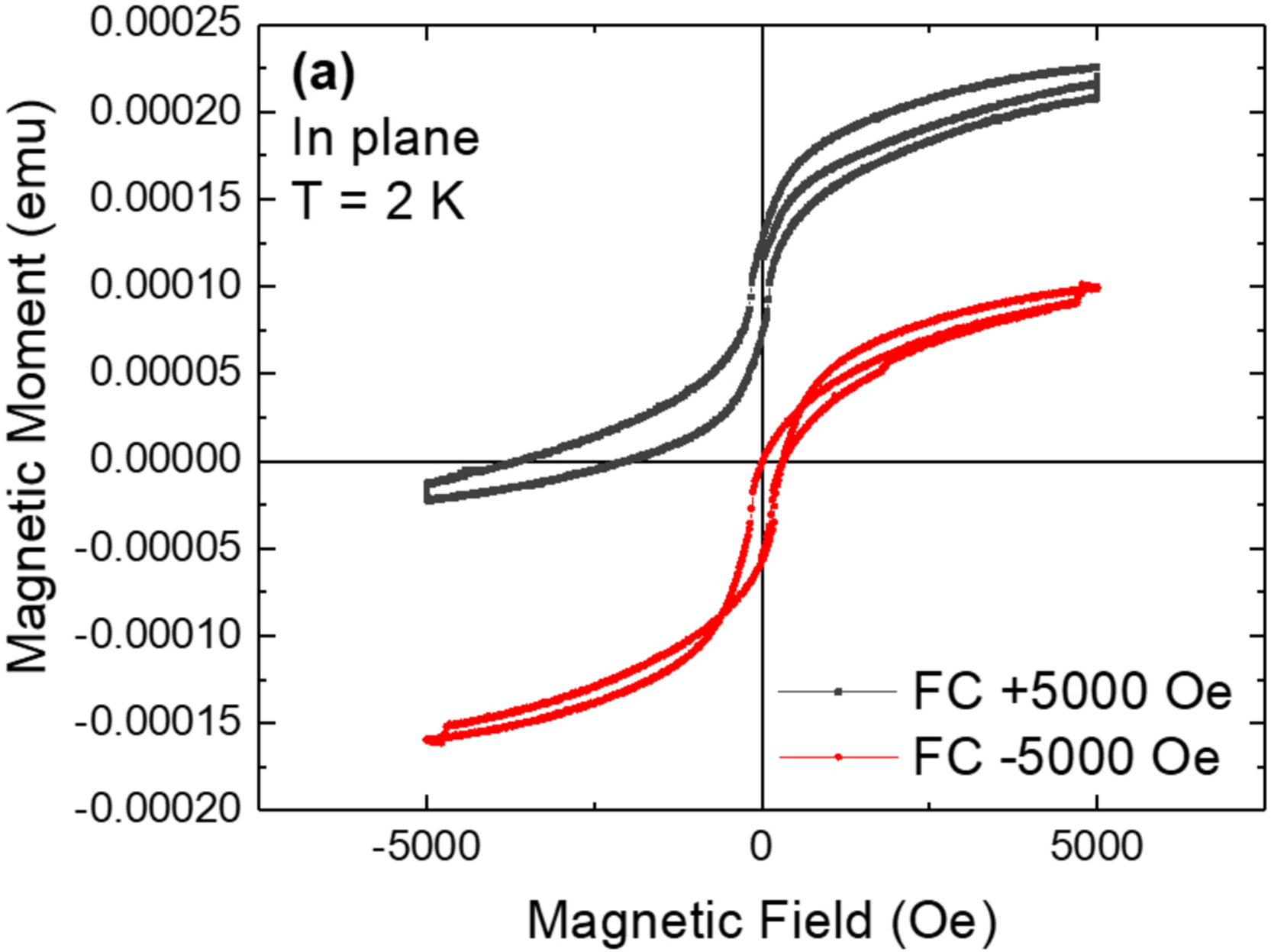
(a)
In plane
T = 2 K
Magnetic Moment (emu)
0.00025
0.00020
0.00015
0.00010
0.00005
0.00000
-0.00005
-0.00010
-0.00015
-0.00020
-5000
0
5000
Magnetic Field (Oe)
FC +5000 Oe
FC -5000 Oe

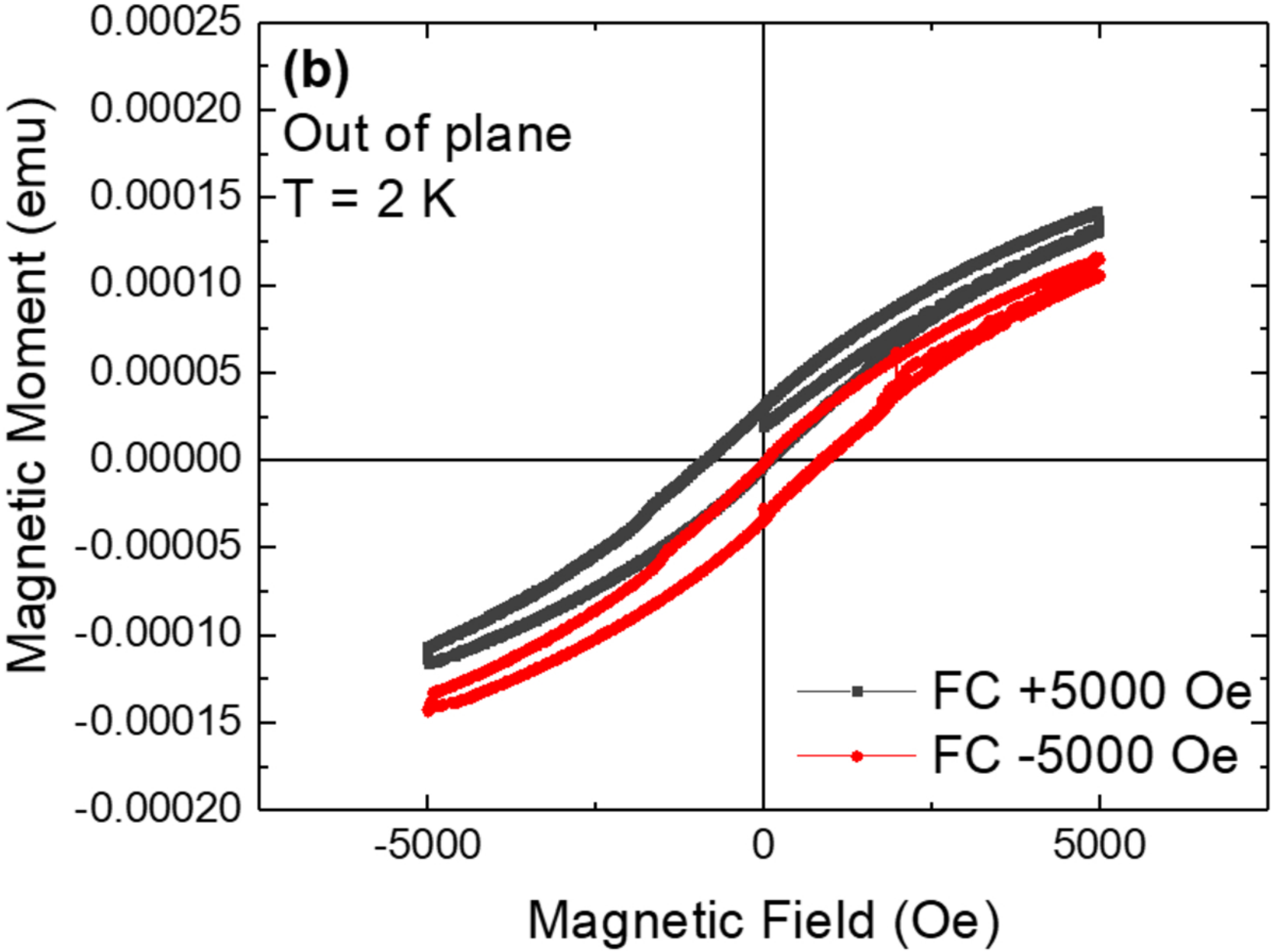
(b)
Out of plane
T = 2 K
Magnetic Moment (emu)
0.00025
0.00020
0.00015
0.00010
0.00005
0.00000
-0.00005
-0.00010
-0.00015
-0.00020
-5000
0
5000
Magnetic Field (Oe)
FC +5000 Oe
FC -5000 Oe